

Non-equilibrium effects in transport through quantum dots

E. Bascones¹, C. P. Herrero¹, F. Guinea¹ and Gerd Schön^{2,3}

¹*Instituto de Ciencia de Materiales, Consejo Superior de Investigaciones Científicas, Cantoblanco, E-28049, Madrid, Spain*

²*Institut für Theoretische Festkörperphysik, Universität Karlsruhe, 76128 Karlsruhe, Germany*

³*Forschungszentrum Karlsruhe, Institut für Nanotechnologie, 76021 Karlsruhe, Germany*

(October 30, 2018)

The role of non-equilibrium effects in the conductance through quantum dots is investigated. Associated with single-electron tunneling are shake-up processes and the formation of excitonic-like resonances. They change qualitatively the low temperature properties of the system. We analyze by quantum Monte Carlo methods the renormalization of the effective capacitance and the gate-voltage dependent conductance. Experimental relevance is discussed.

PACS numbers: 73.40Gk, 73.23.Hk

I. INTRODUCTION.

Quantum dots are paradigms to study the transition from macroscopic to microscopic physics. At present, the role of single-electron charging is well understood [1]. Processes which otherwise are found in solids at the single-atom level, such as the Kondo effect, are being currently investigated [2]. Other atomic features, like the existence of high spin ground states have also been observed [3]. The existence of many internal degrees of freedom within the dot leads to a variety of effects reminiscent of those found in large molecules. Shake-up processes, associated with the rearrangement of many electronic levels upon the addition of one electron, have been reported [4–6].

In the present work, we will show that internal excitations of the dot lead to non-equilibrium effects which can substantially modify the transport properties. In sufficiently small dots, the addition of a single electron may cause significant charge rearrangements [7], and the resulting change in the electrostatic potential of the dot modifies the electronic level structure. In the limit when the level separation is much smaller than other relevant scales, this process leads to an “orthogonality catastrophe” [8], first discussed in relation with the sudden switching of a local potential in a bulk metal. In addition, an electron tunneling event changing the charge of the dot is associated with a charge depletion in the leads or in neighboring dots. The attraction between the electron in the dot and the induced positive charge leads to the formation of an excitonic resonance, similar to the well known excitonic effects in X-ray absorption [9,10].

The relevance of these effects for tunneling processes in mesoscopic systems was first discussed in refs. [11,12] (see also [13]). The existence of excitonic-like resonances has indeed been reported in mesoscopic systems [14]. The formation of bonding resonances has been observed in double well systems [15]. Non-equilibrium effects like those studied here have also been discussed in Ref. [16] where transport through a tunnel junction via localized levels due to impurities was analyzed, and have been observed experimentally in Ref. [17]. A different way for modifying the conductance of quantum dots through the

formation of excitonic states has been proposed in [18]. In that case the exciton is a real bound state, while the excitonic mechanism discussed here is a dynamical process. In some devices, the charge rearrangement may take place far from the tunneling region. In this case no excitons are formed but the orthogonality catastrophe persists. This process has been discussed in relation to the measurement of the charge in a quantum dot by the current through a neighboring point contact [19].

We will study the simplest deviations from the standard Coulomb blockade regime. Our analysis is valid for quantum dots where the spacing between electronic levels, $\Delta\epsilon$, is much smaller than the charging energy, E_C , or the temperature T . The non-equilibrium effects discussed here will be observable if, in addition, the number of electrons in the dot is not too large so that changes in the charge state lead to non-uniform redistributions of the charge. Thus, we will consider an intermediate situation between the Kondo regime and orthodox Coulomb blockade (see below for estimates). The processes that we consider will be present in double-dot devices, but, for definiteness, we study here a single dot.

The main features discussed above can be described by a generalization of the dissipative quantum rotor model [12], which has been studied widely in connection with conventional Coulomb blockade processes [20]. We present a detailed numerical analysis of the generalized model, along similar lines as previous work by some of us on the dissipative quantum rotor [21].

The paper is organized as follows: In the next section, we show how to estimate the parameters which characterize non-equilibrium effects. The model is reviewed in section III, with emphasis on details needed for the subsequent calculations. The numerical method is presented in section IV. In Secs. V and VI, we give results for the renormalized capacitance and conductance. In Sec. VII we discuss some possible experimental evidence of the effects studied here. We close with some conclusions.

II. NON-EQUILIBRIUM EFFECTS.

A. Inhomogeneous charge redistribution.

The standard Coulomb blockade model assumes that, upon a change in the charge state of the dot, the electronic levels within a quantum dot are rigidly shifted by the charging energy, $E_C = e^2/2C$ with C the capacitance of the dot. Deviations from this assumption have been studied by means of an expansion in terms of g^{-1} , the inverse dimensionless conductance, $g \sim k_F l$, where k_F is the Fermi wave-vector, and l is the mean free path [22]. It is also assumed that k_F is small compared to the inverse Thomas-Fermi screening length, $k_{TF} = \sqrt{4\pi e^2 N(\epsilon_F)/\epsilon_0}$. To lowest order beyond standard Coulomb blockade effects, the change in the charge state of the dot leads to an inhomogeneous potential, and induces a term in the Hamiltonian, which can be written as [22,23]:

$$\mathcal{H}_{\text{int}} = (Q - Q_{\text{offset}}) \int \psi^\dagger(\vec{r}) U(\vec{r}) \psi(\vec{r}) d^d \mathbf{r}. \quad (1)$$

Here Q_{offset} denotes offset charges in the environment, the operator Q measures the total electronic charge in the dot, and $\psi^\dagger(\vec{r})$ creates an electron at position \vec{r} . The potential $U(\vec{r})$ modifies the constant shift of the energy levels of the dot assumed in the standard Coulomb blockade model. It appears due to the restricted geometry of the dot. After a charge tunnels into the dot, a pile-up of electrons at the surface of the dot is induced. As a result there is a net attraction of electrons towards the surface, besides a constant shift given by $e^2/2C$. In general, the potential U in eq. (1) can be obtained from the Hartree approximation (in the Thomas-Fermi limit) for dots and leads of arbitrary shape. For a spherical dot of radius R the potential $U(\vec{r})$ has the simple form [22]:

$$U(\vec{r}) = -\frac{e^2 e^{-k_{FT}(R-r)}}{\epsilon_0 k_{TF} R^2} + K \quad (2)$$

and, for a two-dimensional circular dot:

$$U(\vec{r}) = -\frac{e^2}{2\epsilon_0 k_{TF} R \sqrt{R^2 - r^2}} + K. \quad (3)$$

K is a constant which ensures $\langle U(\vec{r}) \rangle = 0$. Non-equilibrium effects arise because the potential in eq. (1) is time dependent, as it changes upon the addition of electrons to the dot. Hamiltonians with terms such as eq. (1) were first discussed in [12] (see next section). Note that the potential is localized in the surface region, where the tunneling electron is supposed to land. Finally, the potential is attractive, leading to the localization of the new electron near the surface, giving rise to excitonic effects.

Other non-equilibrium effects can arise if the charge of the dot induces inhomogeneous potentials in other metallic regions of the device. In this case, the only effect expected is the orthogonality catastrophe (see below), due to the shake-up of the electrons both in the dot and in the other regions. We take this possibility into account in the analysis in the following sections.

B. Effective tunneling density of states.

In the absence of non-equilibrium effects, the conductance of a junction between the dot and the leads is

$$g = \frac{2e^2}{h} \sum_{\text{channels}} |t_i|^2 N_{i,\text{lead}}(E_F) N_{i,\text{dot}}(E_F), \quad (4)$$

where the summation is over the channels, t_i is the hopping matrix element through channel i , $N(E_F)$ is the density of states at the Fermi level, and we use the standard theory of tunneling in the weak transmission limit [24]. Eq. (4) implicitly assumes a constant density of states, as appropriate for a metallic contact.

The non-equilibrium effects to be considered can be taken into account through a modification of the effective tunneling density of states [12,25]. In this case the electron propagators in eq. (4) are the non-equilibrium ones, in an analogous way to the modifications required in the study of X-ray absorption spectra of core levels in metals [9], or tunneling between Luttinger liquids [26–28]. As in those problems, we can distinguish two cases:

i) The analogue of the X-ray absorption process: The charging of the dot leads to an effective potential which modifies the electronic levels. At the same time, an electronic state localized in a region within the range of the potential is filled. The interaction between the electron in this state and the induced potential must be taken into account (the excitonic effects, in the language of the Mahan-Nozières-de Dominicis theory).

ii) The analogue of X-ray photoemission: The charging process leads to a potential which modifies the electronic levels. The tunneling electron appears in a region outside the range of this potential. Only the orthogonality effect caused by the potential needs to be included.

Taking into account the distinctions between these two possibilities, the effective (non-equilibrium) density of states in the lead and the dot becomes (omitting the channel index, i):

$$D_{\text{eff}}(\omega) = \int_0^\omega d\omega' N_{\text{dot}}^{\text{empty}}(\omega') N_{\text{lead}}^{\text{occ}}(\omega - \omega') \propto |\omega|^{1-\epsilon} \quad (5)$$

with ϵ given by

$$\epsilon = \begin{cases} \sum_{j=1,2} 2 \frac{\delta_j}{\pi} - \left(\frac{\delta_j}{\pi}\right)^2 & \text{(excitonic resonance)} \\ -\sum_{j=1,2} \left(\frac{\delta_j}{\pi}\right)^2 & \text{(orthogonality catastrophe)} \end{cases} \quad (6)$$

Here δ_j is the phase shift induced by the new electrostatic potential in the lead states ($j = 1$) or in the dot states ($j = 2$). The exponent is positive, $\epsilon > 0$, if excitonic effects prevail, while $\epsilon < 0$ if the leading process is the orthogonality catastrophe.

We can get an accurate estimate for ϵ in the simple cases of a spherical or circular quantum dot decoupled from other metallic regions discussed in [22]. We assume that tunneling takes place through a single channel, and the contact is of linear dimensions $\propto k_F^{-1}$. In Born approximation the effective phase shift becomes:

$$\delta \approx N(\epsilon_F) \int_{\Omega} U(\vec{r}) d^d \mathbf{r} \approx \begin{cases} \frac{e^2 N(\epsilon_F)}{\epsilon_0 k_{FT} k_F^3 R^2} & \text{spherical dot} \\ \frac{e^2 N(\epsilon_F)}{\epsilon_0 k_{FT} k_F R} & \text{circular dot} \end{cases} \quad (7)$$

where Ω is the region where tunneling processes to the leads are non negligible, typically of dimensions comparable to k_F^{-1} . Note that, for a very elongated dot ($d=1$), the phase shift will not depend on its linear size. As mentioned earlier, the leads can modify significantly these estimates. The tunneling electron can be attracted to the image potential that it induces, enhancing the excitonic effects ($\epsilon > 0$). On the other hand, shake-up processes in metallic regions decoupled from the tunneling processes will increase the orthogonality catastrophe, without contributing to the formation of the excitonic resonance at the Fermi energy.

III. THE MODEL.

The shake-up processes mentioned in the preceding section are described by the Hamiltonian [12]:

$$\begin{aligned} \mathcal{H} &= \mathcal{H}_Q + \mathcal{H}_R + \mathcal{H}_L + \mathcal{H}_T + \mathcal{H}_{int} \\ \mathcal{H}_Q &= \frac{(Q - Q_{offset})^2}{2C} \\ \mathcal{H}_i &= \sum_k \epsilon_{k,i} c_{k,i}^\dagger c_{k,i}, \quad i = L, R \\ \mathcal{H}_T &= t e^{i\phi} \sum_{k,k'} c_{k,R}^\dagger c_{k',L} + h.c. \\ \mathcal{H}_{int} &= (Q - Q_{offset}) \sum_{k,k'} \left(V_{k,k'}^R c_{k,R}^\dagger c_{k',R} - V_{k,k'}^L c_{k,L}^\dagger c_{k',L} \right) \end{aligned} \quad (8)$$

Here $[\phi, Q] = ie$. The Hamiltonian separates the junction degrees of freedom into a collective mode, the charge Q , and the electron degrees of freedom of the electrodes and the dot. This separation is standard in analyzing electron liquids, where collective charge oscillations (the plasmons) are treated separately from the low-energy electron-hole excitations. In our case, this implies that only those states with energies lower than the charging energy are to be included in \mathcal{H}_i , \mathcal{H}_T and \mathcal{H}_{int} in eq.(8). Higher electronic states contribute to the dynamics of the charge, described by \mathcal{H}_Q . The Hamiltonian, eq.(8), suffices to describe transport processes at voltages and temperatures smaller than the charging energy.

In the following, we will express the offset charge Q_{offset} , introduced in eq. (1), by the dimensionless parameter $n_e = Q_{offset}/e$. By $V_{k,k'}$ we denote the matrix elements of $U(\vec{r})$ in the basis of the eigenfunctions near the Fermi level. We allowed that inhomogeneous potentials can be generated on both sides of the junction. We assume that tunneling can take place through several channels (index channel has been omitted). The transmission through each channel should be small for perturbation theory to apply.

The electrical relaxation associated with the tunneling process takes place in two stages. In the first, the tunneling electron is screened by the excitation of plasmons, forming the screened Coulomb potential. The time scale for this process is of the order of the inverse plasma frequency. Next, the screened Coulomb potential excites electron-hole pairs. As the electrons at the Fermi level have a much longer response time, they feel this change as a sudden and local perturbation.

We will restrict ourselves to the regime where the level spacing is small, $\Delta\epsilon \ll T, E_C$. Using standard techniques [20,29], we can integrate out the electron-hole pairs and describe the system in terms of the phase ϕ and charge Q only. This procedure leads to retarded interactions which are long-range in time, as the electron-hole pairs have a continuous spectrum down to zero energy. It is best to describe the resulting model within a path-integral formalism. Because of the non-equilibrium effects the effective action is a generalization of that derived for tunnel junctions [24,29]

$$\begin{aligned} \mathcal{S}[\phi] &= \int_0^\beta d\tau \frac{1}{4E_C} \left(\frac{\partial\phi}{\partial\tau} \right)^2 + \\ &\alpha \int_0^\beta d\tau \int_0^\beta d\tau' E_C^\epsilon \left(\frac{\pi}{\beta} \right)^{2-\epsilon} \frac{1 - \cos[\phi(\tau) - \phi(\tau')]}{\sin^{2-\epsilon}[\pi(\tau - \tau')/\beta]} \end{aligned} \quad (9)$$

It describes the low energy processes below an upper cutoff of order of the unscreened charging energy, E_C . The parameter $\alpha \propto t^2 N_R(\epsilon_F) N_L(\epsilon_F)$ is a measure of the high temperature conductance, g_0 , in units of e^2/h :

$$\alpha = \frac{g_0}{4\pi^2(e^2/h)}. \quad (10)$$

Note that the definition of the action, eq. (9), does not allow us to study temperatures much higher than E_C . The kernel which describes the retarded interaction is given by the effective tunneling density of states, eq. (5). The value of ϵ is the anomalous exponent in the tunneling density of states, given in eq. (5).

The action (9) has been studied extensively for $\epsilon = 0$ [20,21,30,31], describing charging effects in the single-electron transistor in the usual limit where the electrodes are assumed to be in equilibrium. If $\epsilon > 0$, the model has a non-trivial phase transition [32–34]. In this case, for $\alpha > \alpha_{crit} \sim 2/(\pi^2\epsilon)$, the system develops long-range order when $T = 1/\beta \rightarrow 0$, leading to phase coherence and a diverging conductance.

IV. COMPUTATIONAL METHOD

For a given offset charge n_e , the grand partition function can be written in terms of the phase ϕ , as a path integral [20]:

$$Z(n_e) = \sum_{m=-\infty}^{\infty} \exp(2\pi i m n_e) \int \mathcal{D}\phi \exp(-S[\phi]) \quad , \quad (11)$$

where m is the winding number of ϕ , and the paths $\phi(\tau)$ satisfy in sector m the boundary condition $\phi(\beta) = \phi(0) + 2\pi m$.

The effective action and partition function can be rewritten in terms of the phase fluctuations $\theta(\tau) = \phi(\tau) - 2\pi m\tau/\beta$, with boundary condition $\theta(\beta) = \theta(0)$, in the form

$$Z = \sum_{m=-\infty}^{\infty} \exp(2\pi i m n_e) I_m(\alpha, \epsilon, \beta) \quad . \quad (12)$$

The coefficients $I_m(\alpha, \epsilon, \beta) = \int \mathcal{D}\theta \exp(-S_m[\theta])$ are to be evaluated with the effective action $S_m[\theta(\tau)] = S[\theta(\tau) + 2\pi m\tau/\beta]$. They depend on the winding number m , the temperature, and the dimensionless parameters α and ϵ , but are independent of the offset charge n_e . This means that the problem reduces, from a computational point of view, to the calculation of the relative values of $I_m(\alpha, \epsilon, \beta)$, which can be obtained from Monte Carlo (MC) simulations apart from an overall normalization constant [21,31]. The partition function is even and periodic with respect to n_e , $Z(n_e) = Z(-n_e) = Z(n_e + 1)$, and therefore one can restrict the analysis to the range $0 \leq n_e \leq 0.5$.

The MC simulations have been carried out by the usual discretization of the quantum paths into N (Trotter number) imaginary-time slices [35]. In order to keep roughly the same precision in the calculated quantities, as the temperature is reduced, the number of time-slices N has to increase as $1/T$. We have found that a value $N = 4\beta E_C$ is sufficient to reach convergence of I_m . Therefore, the imaginary-time slice employed in the discretization of the paths is $\Delta\tau = \beta/N = 1/(4E_C)$.

When discretizing the paths $\phi(\tau)$ into N points, it is important to treat correctly the $|\tau - \tau'| \rightarrow 0$ divergence that appears in the tunneling term $S_t[\phi]$ of the effective action [second term on the r.h.s. of Eq.(9)]. This divergence can be handled as follows. In the discretization procedure, the double integral in $S_t[\phi]$ translates into a sum extended to N^2 two-dimensional plaquettes, each one with area $(\Delta\tau)^2$. The above-mentioned divergence appears in the N “diagonal” terms ($\tau = \tau'$) and can be dealt with by approximating the integrand close to $\tau = \tau'$ by $E_C^\epsilon |\tau - \tau'|^\epsilon (d\phi/d\tau)^2/2$. Thus, by integrating this expression over the “diagonal” plaquette (i, i) , with $1 \leq i \leq N$, one finds that its contribution to $S_t[\phi]$ is given by

$$\Delta S_t(\tau_i, \tau_i) = 2 E_C^\epsilon \frac{\alpha}{\epsilon + 1} \left(\frac{\Delta\tau}{2} \right)^{\epsilon+2} \left(\frac{d\phi}{d\tau} \right)_{\tau=\tau_i}^2 \quad , \quad (13)$$

which is regular for $\epsilon \neq -1$. The error introduced by this replacement in the discretization procedure is of the same order as that introduced by the usual discretization of the “non-diagonal” terms. We have checked that the results of our Monte Carlo simulations obtained by using this procedure converge with the Trotter number N .

The partition function in Eq.(12) has been sampled by the classical Metropolis method [36] for temperatures down to $k_B T = E_C/200$. A simulation run proceeds via successive MC steps. In each step, all path-coordinates (imaginary-time slices) are updated. For each set of parameters (α, ϵ, T) , the maximum distance allowed for random moves was fixed in order to obtain an acceptance ratio of about 50%. Then, we chose a starting configuration for the MC runs after system equilibration during about 3×10^4 MC steps. Finally, ensemble-averaged values for the quantities of interest were calculated from samples of $\sim 1 \times 10^5$ quantum paths. More details on this kind of MC simulations can be found elsewhere [21].

V. RENORMALIZATION OF THE CAPACITANCE.

We will study the capacitance renormalization for tunneling conductance $\alpha > 0$ by calculating the effective charging energy $E_C^*(T) = e^2/2C^*(T)$, which can be obtained as a second derivative of the free energy $F = -k_B T \ln Z$:

$$E_C^*(T) = \frac{1}{2} \left. \frac{\partial^2 F}{\partial n_e^2} \right|_{n_e=0} \quad . \quad (14)$$

At high temperatures, the free energy $F(n_e)$ depends weakly on n_e , and the curvature [i.e., $E_C^*(T)$] approaches zero. At low T , and for weak tunneling ($\alpha \ll 1$), it coincides with the usual charging energy E_C . By using Eqs. (11) and (14) this renormalized charging energy can readily be expressed as

$$E_C^*(T) = 2\pi^2 k_B T \langle m^2 \rangle_{n_e=0} \quad , \quad (15)$$

where $\langle m^2 \rangle_{n_e=0}$ is the second moment of the coefficients I_m .

The correlation function in imaginary time $G(\tau)$, that will be used below to calculate the conductance, can be calculated from the MC simulations as $G(\tau) = \langle \cos[\phi(\tau) - \phi(0)] \rangle$. This means in our context:

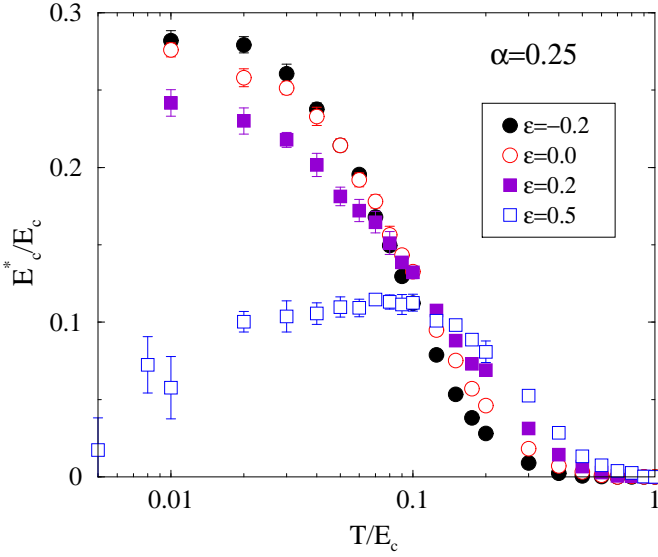


FIG. 1. Effective charging energy of the single electron transistor for different values of ϵ and $\alpha = 0.25$, as a function of temperature.

$$G(\tau) = \frac{1}{Z} \sum_{m=-\infty}^{\infty} \exp(2\pi i m n_e) \times \int \mathcal{D}\phi e^{-S[\phi]} \cos[\phi(\tau) - \phi(0)] . \quad (16)$$

A number of features, directly related to the free energy of the model given by action (9), are reasonably well understood for $\epsilon = 0$. The effective charge induced by an arbitrary offset charge, n_e , has been extensively analyzed. A number of analytical schemes give consistent results in the weak coupling ($\alpha \ll 1$) regime [37,38]. These calculations have been extended to the strong coupling limit by numerical methods [21].

In fig. (1), we present results for the effective charging energy E_C^* as a function of temperature, and for different values of ϵ . The value of E_C^* is enhanced for $\epsilon < 0$, where the orthogonality catastrophe dominates the physics. A positive ϵ reduces the effective charging energy, and, beyond some critical value (see discussion below), E_C^* scales towards zero as the temperature is decreased, showing non-monotonic behavior. The same trend can be appreciated in fig. (2), where the effective charging energy at low temperatures is plotted as a function of α . Renormalization group arguments [32,33] show that $E_C^*(\alpha, \epsilon)$ should go to zero for $\alpha > \alpha_{crit}(\epsilon)$. We have checked the consistency of this prediction with the numerical results by fitting the values of $E_C^*(\alpha)$ at low temperatures by the expression expected from the scaling analysis near the transition [32]:

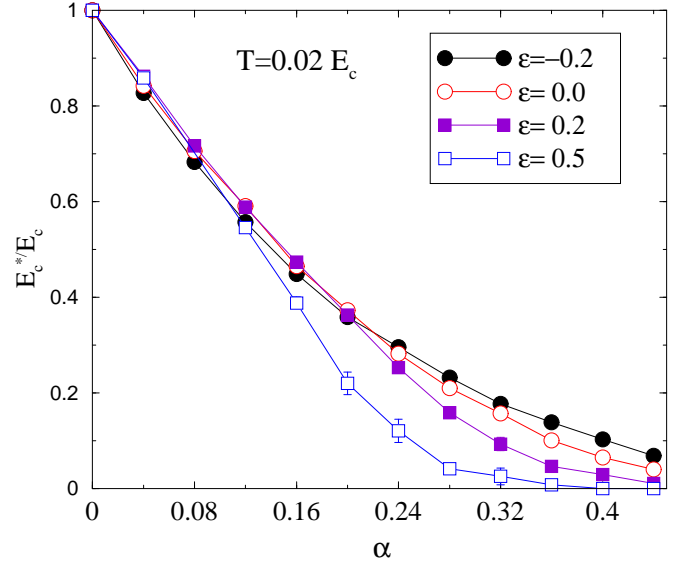


FIG. 2. Effective charging energy of the single electron transistor for different values of ϵ , as a function of α for $T/E_C = 0.02$.

$$E_C^*(\alpha, \epsilon) = \left[1 - \frac{\alpha}{\alpha_{crit}(\epsilon)} \right]^{\frac{1}{\epsilon}} \quad (17)$$

In this expression we use $\alpha_{crit}(\epsilon)$ as the only adjustable parameter. The results are shown in fig. (3). Note that the same equation (17) can be used to fit the results for $\epsilon < 0$, if one uses a negative value for α_{crit} . There is no phase transition, however, for $\epsilon < 0$.

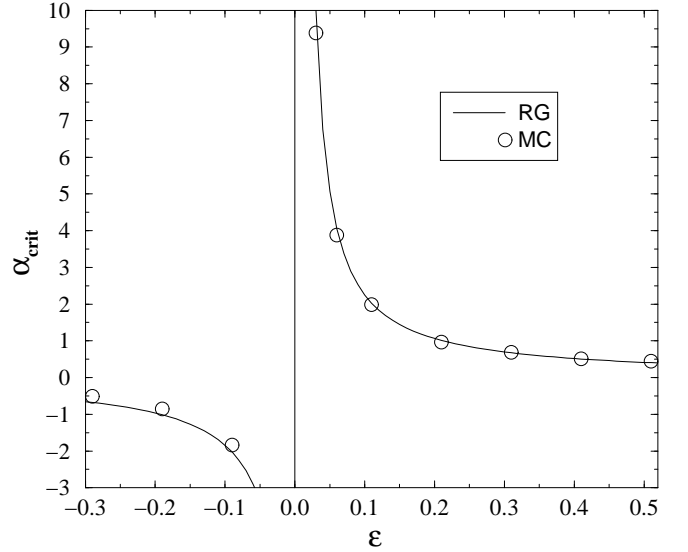


FIG. 3. Critical line determined by the RG calculation: $\alpha_{crit} = 2/(\pi^2 \epsilon)$ and values calculated fitting the numerical data for $E_C^*(\alpha, \epsilon)$ to the expression (17).

The results show that the present calculations are very accurate even for relatively large values of α , where E_C^* converges at very low temperatures.

VI. EVALUATION OF THE CONDUCTANCE.

A. $\epsilon = 0$

The conductance of the single-electron transistor is notoriously more difficult to calculate than standard thermodynamic averages. It cannot be derived in a simple fashion from the partition function, and requires the analytical continuation of the response functions from imaginary to real times or frequencies [39]. Hence, there are no comprehensive results valid for the whole range of values of $\alpha, T/E_C$ and n_e . For $\epsilon = 0$, the conductance $g(T)$ can be written as [40–42]:

$$g(T) = 2g_0\beta \int_0^\infty \frac{d\omega}{2\pi} \frac{\omega S(\omega)}{e^{\beta\omega} - 1} \quad (18)$$

where g_0 is the normal state conductance, and $S(\omega)$ is related to the correlation function in imaginary time [43]:

$$\begin{aligned} G(\tau) &= \langle e^{i\phi(\tau)} e^{-i\phi(0)} \rangle \\ &= \frac{1}{2\pi} \int_0^\infty d\omega \frac{e^{(\beta-\tau)\omega} + e^{\tau\omega}}{e^{\beta\omega} - 1} A(\omega) \end{aligned} \quad (19)$$

and

$$A(\omega) = (1 - e^{-\beta\omega})S(\omega) \quad (20)$$

In the previous expressions, the charging energy is the natural cutoff for the energy integrals.

At high temperatures, $\beta E_C \sim 1$, we can expand in eq. (18):

$$g(T) \approx 2g_0\beta \int_0^\infty \frac{d\omega}{2\pi} \left[\frac{1}{\beta} - \frac{\beta\omega^2}{24} + \frac{7\beta^3\omega^4}{5760} + \dots \right] \frac{e^{(\beta\omega)/2} A(\omega)}{e^{\beta\omega} - 1} \quad (21)$$

so that:

$$g(T) \approx g_0 \left[G\left(\frac{\beta}{2}\right) - \frac{\beta^2}{24} G''\left(\frac{\beta}{2}\right) + \frac{7\beta^4}{5760} G^{iv}\left(\frac{\beta}{2}\right) + \dots \right] \quad (22)$$

At low temperatures, $\beta E_C \gg 1$, the conductance is dominated by the low energy behavior of $A(\omega)$ or, alternatively, $S(\omega)$. To lowest order, we expect an expansion of the form:

$$S(\omega) \approx 2\pi\delta(\omega - \omega_0) + A|\omega| + \dots \quad (23)$$

where ω_0 is an energy of the order of the renormalized charging energy (or zero at resonance, $n_e \approx 1/2$), and A is a constant which describes cotunneling processes [44]. Inserting this expression in eq. (18), we obtain:

$$g(T) \approx g_0 \frac{2\beta\omega_0}{e^{\beta\omega_0} - 1} + g_0 \frac{A}{\pi\beta^2} \int_0^\infty dx \frac{x^2}{e^x - 1} + \dots \quad (24)$$

while, on the other hand:

$$G\left(\frac{\beta}{2}\right) \approx 2e^{-\frac{1}{2}\beta\omega_0} + \frac{A}{\pi} \left(\frac{2}{\beta}\right)^2 + \dots \quad (25)$$

If $\omega_0 = 0$, both g and $g_0 G(\beta/2)$ have the same limit, as $T \rightarrow 0$. When $\omega_0 \neq 0$ the leading term goes as T^2 (cotunneling) in both cases, with prefactors equal to $2.404A/\pi$ and $4A/\pi$, respectively.

From the above discussion of the relation between the high- and low-temperature behavior of $g(T)$ and $G(\beta/2)$, we find that the interpolation formula

$$g(T) \approx g_0 G\left(\frac{\beta}{2}\right) \quad (26)$$

should give a reasonable approximation over the entire range of parameters (note that the above discussion is independent of the values of α and n_e). Eq. (26) is consistent with the the main physical features expected both in the high and low temperature limits, at and away from resonance. The advantage of using $G(\beta/2)$ is that it can be computed, to a high degree of accuracy, by standard Monte Carlo techniques, as it does not require to continue the results to real times. A similar approximation, used to avoid inaccurate analytical continuations has been applied for bulk systems in Ref. [45].

We show the adequacy of the approximation, eq. (26), by plotting the conductances estimated in this way, as a function of the bias charge n_e , in fig. (4).

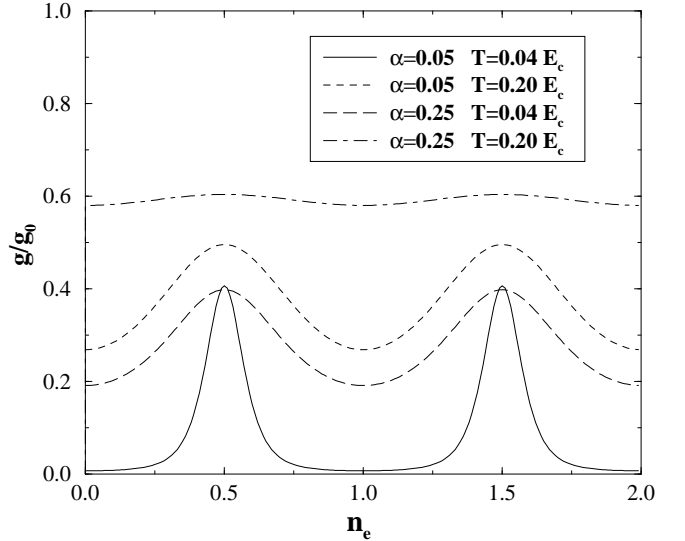


FIG. 4. Conductance of the single-electron transistor ($\epsilon = 0$), as a function of the dimensionless bias charge n_e , for several values of the coupling α , and two different temperatures.

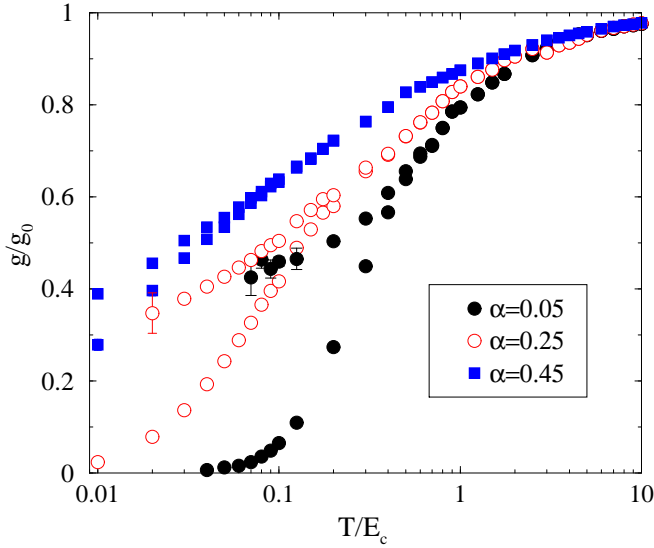


FIG. 5. Maximum and minimum values of the conductance of the single-electron transistor ($\epsilon = 0$), as a function of temperature, for different values of the coupling α .

The minimum ($n_e = 0$) and maximum conductances ($n_e = 1/2$) for different values of α and temperatures are shown in fig. (5).

B. $\epsilon \neq 0$

We now extend the previous approximation to the conductance, eq. (26) to the case $\epsilon \neq 0$. The main modification in eq. (18) is that a factor $\omega/(1 - e^{-\beta\omega})$ within the integral has to be replaced by the effective tunneling density of states, D_{eff} , given, at zero temperature, by eq. (5). At finite temperatures, the corresponding expression is approximately

$$D_{\text{eff}}(\omega) \propto \max[T(T/E_C)^{-\epsilon}, \omega(\omega/E_C)^{-\epsilon}]. \quad (27)$$

The relevant range in the integrand in eq. (18) is from $\omega = 0$ to $\omega \approx T$. In the following, we will factor the ϵ dependent part of the effective density of states, and we write the generalization of eq. (5) to finite temperatures as:

$$D_{\text{eff}}(\omega) = \frac{\omega}{1 - e^{-\beta\omega}} D_{\text{res}}(\epsilon, \omega) \quad (28)$$

Finally, when inserting this expression into eq. (18), we make the approximation:

$$D_{\text{res}}(\epsilon, \omega) \approx \left(\frac{T}{E_C}\right)^{-\epsilon} \quad (29)$$

With this approximation, we can perform the same analysis in the high and low temperature regimes as before, to obtain the interpolation formula:

$$g(T) \approx g_0 \left(\frac{T}{E_C}\right)^{-\epsilon} G\left(\frac{\beta}{2}\right) \quad (30)$$

This expression includes again the relevant physical processes at high and low temperatures.

Results for the maximum and minimum values of the conductances, for different values of ϵ , are presented in fig. (6). In the non phase-coherent regime, at very low temperatures, $T \ll E_C^*$, the conductance away from resonance should vary as $g \propto T^{2-2\epsilon}$. Exactly at resonance, $n_e = 1/2$, the conductance diverges as $T^{-\epsilon}$. The most interesting result is the divergence of the conductance, at low temperatures, for $\epsilon = 0.5$, where the excitonic effects are strong enough to drive the system to the phase-coherent phase.

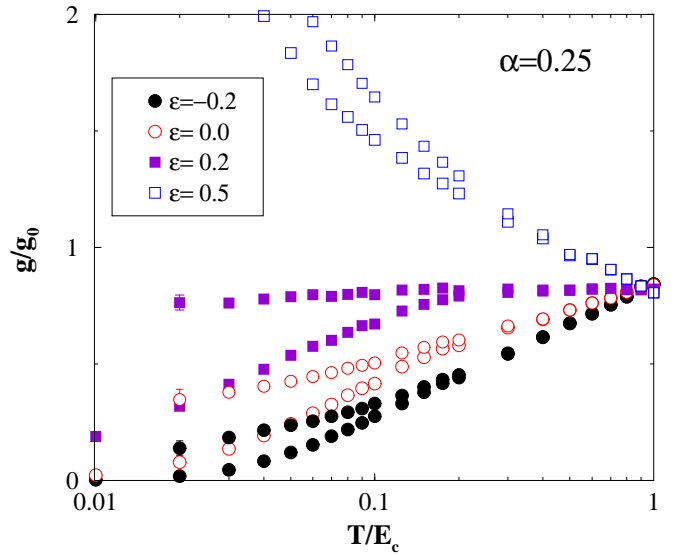


FIG. 6. Maximum and minimum values of the conductance of the single-electron transistor, for different values of ϵ .

The full conductance, as a function of n_e , is shown in fig. (7), for $\alpha = 0.25$ and $\epsilon = 0.5$. As mentioned above, for these parameters the system is already in the phase coherent regime. The conductance behaves in a way similar to that in the usual case ($\epsilon = 0$), and a peaked structure develops. The absolute magnitude, however, increases as the temperature is lowered. Note that the effective charging energy is finite as $T \rightarrow 0$ (see fig. (1)). It is interesting to note that, in this phase with complete suppression of Coulomb blockade effects at low temperatures (high values of ϵ and high conductances), the peak structure appears only for an intermediate range of temperatures, and it is washed out at very low temperatures.

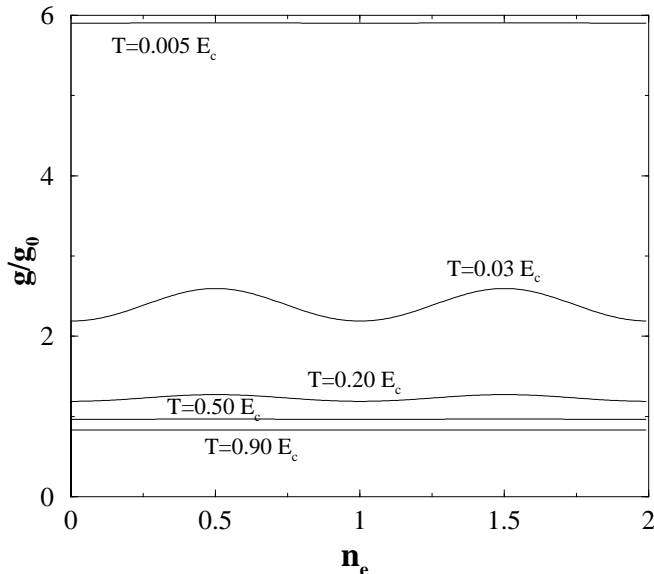


FIG. 7. Conductance, as a function of n_e and temperature, of a single-electron transistor with $\alpha = 0.25$ and $\epsilon = 0.5$.

In fig. (8) we show the conductance as a function of ϵ for a fixed temperature. It is evident the increase of the conductance as ϵ increases.

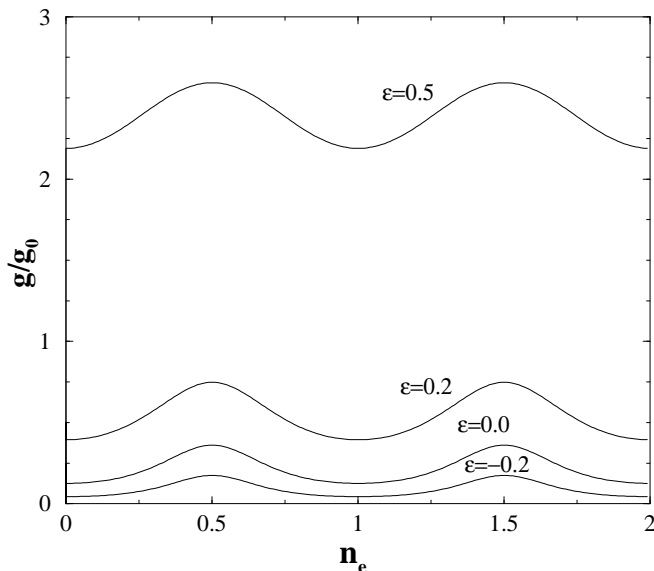


FIG. 8. Conductance, as a function of n_e , of a single-electron transistor with $\alpha = 0.25$ and different values of ϵ ($T = 0.03 E_C$).

VII. DISCUSSION.

In the following, we discuss some experimental evidence which can be explained within the model discussed here.

It has been pointed out [46] that the correlations between the conductances for neighboring charge states of a

quantum dot [47] are too weak to be explained using standard methods for disordered, non-interacting systems. The experiments reported in [47] are in the cotunneling regime. In the presence of non-equilibrium processes, we expect a behavior of the type $g \propto T^{2-2\epsilon}$. Note that ϵ is determined by phase shifts, which depend on microscopic details of the contacts. Thus, it can be expected to vary with the charge state of the dot, and to lead to large differences in the conductances of neighboring valleys.

It has been shown that the temperature dependence of the conductance quantum dots, away from resonances, can be opposite to that expected in a system exhibiting Coulomb blockade [48]. This effect could not be attributed to Kondo physics, as the data do not show an even-odd alternation. The reported behavior can be explained within our model, assuming that the value of ϵ is sufficiently large, and dependent on the charge state of the dot.

In ref. [49] the inelastic contribution to the conductance in a double dot system, where the electronic states in the two dots are separated by an energy ϵ is measured. The result is approximately given by $I_{\text{inel}}(\epsilon) \propto \epsilon^\lambda$, where λ is a negative constant of order unity. Taking into account only one electronic state within each dot, the problem can be reduced to that of a dissipative, biased two level system. The inelastic conductance reflects the nature of the low energy excitations coupled to the two level system. The observed power law decay implies that the spectral strength of the coupling, that is the function $J(\omega)$ in the standard literature [43], should be ohmic, $J(\omega) \propto |\omega|$. This has led to the proposal that the excitations coupled to the charges in the double dot system are piezoelectric phonons [49,50]. It is interesting to note that the excitation of electron-hole pairs leads also to an ohmic spectral function. Thus, at sufficiently low energies, an orthogonality catastrophe due to electron-hole pairs shows a behavior indistinguishable from that arising from piezoelectric phonons. The contributions from the two types of excitations can be distinguished at the natural cutoff scale for phonons, which is the energy of a phonon whose wavelength is of the order of the dimensions of the device. On the other hand, the simplest prediction for the expected behavior of the current induced by the emission of the electron-hole pairs is:

$$I(\epsilon) \propto K \frac{1}{1 - e^{-\beta \sqrt{\Delta_0^2 + \epsilon_b^2}}} \frac{\Delta_0^2}{\sqrt{\Delta_0^2 + \epsilon_b^2}} \quad (31)$$

where Δ_0 is the tunneling element between the two dots, ϵ_b is the bias, and K is the coupling constant (referred to as ϵ in other sections of this paper). This expression gives the absorption rate of a dissipative two level system in the weak coupling regime, $K \ll 1$ [43]. The natural cutoff for electron-hole pairs is bounded by the charging energy of the system. It would be interesting to disentangle the relative contributions of electron-hole pairs and piezoelectric phonons to the inelastic current.

The photo-induced conductance in a double dot system

has also been measured [51]. The analysis of the contribution of inelastic processes due to electron hole pairs to the measured conductance proceeds in the same way as in the interpretation of the previous experiment. Let us suppose that a photon of energy ω_{ph} excites an electron within one dot. Assuming that the coupling to the environment is weak, the rate at which the electron tunnels to the second dot by losing an energy ϵ is given by eq.(31). The experiments in [51] suggest that the number of states within each dot are discrete. Then, the induced conductance should show a series of peaks, related to resonant photon absorption within one dot. The height of each peak is determined by the decay rate to lower excited states in the other dot, and it can be written as a sum of terms with the dependence given in eq.(31), where ϵ is the energy difference between the initial and final states. The envelope of the spectrum should look like a power law, in qualitative agreement with the experiments.

It is interesting to note that bunching of energy levels in quantum dots have been reported [52]. The separation between peaks defines the charging energy, which, according to the experiments, vanishes for certain charge states. This behavior can be explained if the excitonic effects drive the quantum dot beyond the transition, and charging effects are totally suppressed. This mechanism can also play some role in the observed transitions in granular wires [25,53].

VIII. CONCLUSIONS.

We have analyzed the effects of non-equilibrium transients after a tunneling process on the conductance of quantum dots. They are related to the change in the electrostatic potential of the dot upon the addition of a single electron. These effects can enhance or suppress the Coulomb blockade. The most striking effect arise from the formation of an exciton-like resonance at the Fermi level after the charging process and lead to the complete suppression of the Coulomb blockade and a diverging conductance at low temperatures. It appears for sufficiently large values of the conductance, α , and the non-equilibrium phase shifts which define ϵ in our model. The same potential which leads to this dynamic resonance plays a role in the deviations of the level spacings from the standard Coulomb blockade model [22].

For simplicity, we have considered the simplest case, a single-electron transistor. The analysis reported here can be extended, in a straightforward fashion to other devices, like double quantum dots, where the effects described here should be easier to observe.

As discussed, the non-equilibrium effects considered in this paper may have been observed already in the conductance of quantum dots.

IX. ACKNOWLEDGMENTS

One of us (E. B.) is thankful to the University of Karlsruhe for hospitality. We acknowledge financial support from CICYT (Spain) through grant PB0875/96, CAM (Madrid) through grant 07N/0045/1998 and FPI, and the European Union through grant ERBFM-RXCT960042.

-
- [1] see several articles in *Single Charge Tunneling*, H. Grabert and M. H. Devoret eds. (Plenum Press, New York, 1992).
 - [2] D. Goldhaber-Gordon, H. Shtrikman, D. Mahalu, D. Abusch-Magder, U. Meirav and M. A. Kastner, *Nature* **391**, 156 (1998). S. M. Cronenwett, T. H. Oosterkamp and L. P. Kouwenhoven, *Science* **281**, 540 (1998).
 - [3] T. H. Oosterkamp, S. F. Godijn, M. J. Uilenreef, Y. V. Nazarov, N. C. van der Vaart and L. P. Kouwenhoven, *Phys. Rev. Lett.* **80**, 4951 (1998).
 - [4] D. R. Stewart, D. Sprinzak, C. M. Marcus, C. I. Duruöz and J. S. Harris Jr., *Science* **278**, 1784 (1997). S. R. Patel, D. R. Stewart, C. M. Marcus, M. Gökcedag, Y. Alhassid, A. D. Stone, C. I. Duruöz and J. S. Harris Jr., *Phys. Rev. Lett.* **81**, 5900 (1998).
 - [5] T. H. Oosterkamp, J. W. Janssen, L. P. Kouwenhoven, D. G. Austing, T. Honda and S. Tarucha, *Phys. Rev. Lett.* **82**, 2931 (1999).
 - [6] O. Agam, N. S. Wingreen, B. I. Altshuler, D. C. Ralph and M. Tinkham *Phys. Rev. Lett.* **78**, 1956 (1997).
 - [7] U. Sivan, R. Berkovits, Y. Aloni, O. Prus, A. Auerbach and G. Ben-Yoseph, *Phys. Rev. Lett.* **77**, 1123 (1996). P. N. Walker, Y. Gefen and G. Montambaux, *Phys. Rev. Lett.* **82**, 5329 (1999).
 - [8] P. W. Anderson, *Phys. Rev.* **164**, 352 (1967). For a discussion of the orthogonality catastrophe in the context of quantum dots, see K. A. Matveev, L. I. Glazman and H. U. Baranger, *Phys. Rev. B* **54**, 5637 (1996).
 - [9] P. Nozières and C. T. de Dominicis, *Phys. Rev.* **178**, 1097 (1969).
 - [10] G. D. Mahan, *Many-Particle Physics* (Plenum, New York, 1991).
 - [11] M. Ueda and S. Kurihara, in *Macroscopic Quantum Phenomena*, edited by T. D. Clark et al. (World Scientific, Singapore, 1990).
 - [12] M. Ueda and F. Guinea, *Zeits. für Phys. B* **85**, 413 (1991).
 - [13] F. Guinea, E. Bascones and M. J. Calderón in *Lectures on the Physics of Highly Correlated Electrons*, F. Mancini ed., AIP press (New York), 1998.
 - [14] M. Matters, J. J. Versluys and J. E. Mooij, *Phys. Rev. Lett.* **78**, 2469 (1997).
 - [15] N. C. van der Waart, S. F. Godijn, Y. V. Nazarov, C. J. P. M. Harmans, J. E. Mooij, L. W. Molenkamp and C. T. Foxon, *Phys. Rev. Lett.* **74**, 4702 (1995). R. H. Blick, D. Pfannkuche, R. J. Haug, K. v. Klitzing, and

- K. Eberl, Phys. Rev. Lett. **80**, 4032 (1998). T. H. Oosterkamp, T. Fujisawa, W.G. van der Wiel, K. Ishibashi, R.V. Hijman, S. Tarucha and L.P. Kouwenhoven, Nature **395**, 873 (1998).
- [16] K. A. Matveev and A. I. Larkin, Phys. Rev. B **46**, 15337 (1992).
- [17] A. K. Geim, P. C. Main, N. La Scala Jr., L. Eaves, T. J. Foster, P. H. Beton, J. W. Sakai, F. W. Sheard, M. Henini, G. Hill, and M. A. Pate, Phys. Rev. Lett. **72**, 2061 (1994).
- [18] M. Pustilnik, Y. Avishai and K. Kikoin, preprint (cond-mat/9908004), and Physica B, to be published.
- [19] A. Yacoby, M. Heiblum, D. Mahalu and H. Shtrikman, Phys. Rev. Lett. **74**, 4047 (1995). Y. Levinson, Europhys. Lett. **39**, 299 (1997). I. L. Aleiner, N. S. Wingreen, and Y. Meir, Phys. Rev. Lett. **79**, 3740 (1997).
- [20] G. Schön and A. D. Zaikin, Phys. Rep. **198**, 238 (1990).
- [21] C. P. Herrero, G. Schön and A. D. Zaikin, Phys. Rev. B **59**, 5728 (1999).
- [22] Ya. M. Blanter, A. D. Mirlin and B. A. Muzykantskii, Phys. Rev. Lett. **78**, 2449 (1997).
- [23] For a review see L. I. Glazman, **Single electron tunneling**, to be published in a special issue of Journal of Low Temperature Physics .
- [24] E. Ben-Jacob, E. Mottola and G. Schön, Phys. Rev. Lett. **51**, 2064 (1983).
- [25] S. Drewes, S. R. Renn and F. Guinea, Phys. Rev. Lett. **80**, 1046 (1998).
- [26] C. Kane and M. P. A. Fisher, Phys. Rev. B **46**, 15233 (1992).
- [27] K. A. Matveev and L. I. Glazman, Phys. Rev. Lett. **70**, 990 (1993).
- [28] M. Sasseti and B. Kramer, Phys. Rev. B **55**, 9306 (1997).
- [29] V. Ambegaokar, U. Eckern and G. Schön, Phys. Rev. Lett. **48**, 1745 (1982).
- [30] G. Falci, G. Schön, and G.T. Zimanyi, Phys. Rev. Lett. **74**, 3257 (1995).
- [31] X. Wang, R. Egger, and H. Grabert, Europhys. Lett. **38**, 545 (1997).
- [32] J. M. Kosterlitz, Phys. Rev. Lett. **37**, 1577 (1977).
- [33] F. Guinea and G. Schön, J. Low Temp. Phys. **69**, 219 (1986).
- [34] T. Strohm and F. Guinea, Nucl. Phys. B **487**, 795 (1997).
- [35] *Quantum Monte Carlo Methods in Condensed Matter Physics*, edited by M. Suzuki (World Scientific, Singapore, 1993).
- [36] K. Binder and D.W. Heermann, *Monte Carlo Simulation in Statistical Physics* (Springer, Berlin, 1988).
- [37] G. Göppert, H. Grabert, N. Prokof'ev, and B. V. Svistunov, Phys. Rev. Lett. **81**, 2324 (1998).
- [38] J. König and H. Schoeller, Phys. Rev. Lett. **81**, 3511 (1998).
- [39] G. Göppert, B. Hupper and H. Grabert, to be published in Physica B.
- [40] W. Zwerger and M. Scharpf, Z. Phys. B **85**, 421 (1991).
- [41] G. Ingold and A. V. Nazarov in ref. [1].
- [42] G. Göppert and H. Grabert, C.R.Acad. Sci. **327**, 885 (1999). G. Göppert and H. Grabert, cond-mat/9910237
- [43] U. Weiss, *Quantum dissipative systems* (World Scientific, Singapore, 1993).
- [44] D. V. Averin and Yu. V. Nazarov, Phys. Rev. Lett. **65**, 2446 (1990).
- [45] M. Randeria, N. Trivedi, A. Moreo and R. T. Scalettar, Phys. Rev. Lett. **69**, 2001 (1992). N. Trivedi and M. Randeria, Phys. Rev. Lett. **75**, 312 (1995).
- [46] R. Baltin and Y. Gefen, Phys. Rev. Lett. **83**, 5094 (1999).
- [47] S. M. Cronnenwett, S. R. Patel, C. M. Marcus, K. Campman and A. C. Gossard, Phys. Rev. Lett. **79**, 2312 (1997).
- [48] S. M. Maurer, S. R. Patel, C. M. Marcus, C. I. Duruöz and S. J. Harris, Phys. Rev. Lett. **83**, 1403 (1999).
- [49] T. Fujisawa, T.H. Oosterkamp, W.G. van der Wiel, B. Broer, R. Aguado, S. Tarucha, and L.P. Kouwenhoven, Science **282**, 932 (1998).
- [50] T. Brandes and B. Kramer, Phys. Rev. Lett. **83**, 3021 (1999).
- [51] R. H. Blick, D. W. van der Weide, R. J. Haug and K. Eberl, Phys. Rev. Lett. **81**, 689 (1998).
- [52] N. V. Zhitenev, A. C. Ashoori, L. N. Pfeiffer and K. W. West, Phys. Rev. Lett. **79**, 2308 (1997).
- [53] A. V. Herzog, P. Xiong, F. Sharifi and R. C. Dynes, Phys. Rev. Lett. **76**, 668 (1996).